JOURNAL OF PROPULSION AND POWER
Vol. 20, No. 4, July–August 2004

Reflected-Shock Ignition of $SiH_4/H_2/O_2/Ar$ and $SiH_4/CH_4/O_2/Ar$ Mixtures

Eric L. Petersen* and Danielle M. Kalitan†
University of Central Florida, Orlando, Florida 32816
and
Matthew J. A. Rickard‡
The Aerospace Corporation, El Segundo, California 90245

High-temperature experiments were performed behind reflected shock waves with H_2/O_2, $SiH_4/H_2/O_2$, CH_4/O_2, and $SiH_4/CH_4/O_2$ mixtures highly diluted in argon. Reflected-shock temperatures ranged from 1000–2250 K at a pressure near 1 atm. Reaction progress was monitored by observation of the time histories of several species by the use of emission techniques, including OH*, SiH_4, and CH*. The oxidation and ignition data are reported in the form of species concentration profiles and plots of characteristic times as a function of temperature. The presence of silane in the fuel/O_2 mixtures markedly reduced the ignition delay time of all H_2/O_2 and CH_4/O_2 mixtures, usually by a factor of two or more, even at molar SiH_4 concentrations as low as 1% of the fuel concentration. Although the decrease in ignition delay time was, in some cases, quite significant, the activation energy of ignition when plotted on an Arrhenius diagram remained virtually unchanged; this result indicates that the chain-branching behavior that takes place when silane is present, although faster and through different elementary reactions, is similar to the behavior when silane is not present. The addition of silane to H_2/O_2 mixtures also appears to extend the chain-branching kinetics to lower temperatures, eliminating the classic chain termination seen near the second explosion limit of H_2/O_2 ignition.

Introduction

SILANE oxidation and ignition are important in several combustion applications, ranging from high-speed propulsion to materials processing. Because of its hypergolic nature, SiH_4 is of interest as an ignition promoter in advanced airbreathing engines, particularly those requiring the supersonic combustion of hydrocarbon fuels.[1–3] Silane is also a primary source of silicon in the formation of silicon oxides for electronics, semiconductor, and glass applications via the chemical vapor deposition and flame synthesis processes.[4,5] Related efforts to develop comprehensive chemical kinetics mechanisms of silane combustion have appeared in recent years.[6–10]

Although some progress has been made toward understanding the combustion chemistry of silane oxidation and ignition, few quantitative data exist at elevated temperatures (900 K+) for the validation of the detailed chemical kinetics models. Shock tubes are ideal devices for obtaining such combustion chemistry data at high temperatures due to their ease of use, high repeatability, and accurate production of elevated temperatures. In fact, the only available set of quantitative ignition delay time data at elevated temperatures was obtained by McLain et al.[1] using the shock-tube technique. In their study, McLain et al. measured the ignition delay times of two $SiH_4/H_2/O_2/N_2$ mixtures behind reflected shock waves using pressure to determine when ignition occurred over a range of temperatures from approximately 800–1050 K.

Received 17 December 2002; revision received 5 November 2003; accepted for publication 5 November 2003.

*Assistant Professor, Mechanical, Materials, and Aerospace Engineering. Member AIAA.

†Research Assistant, Mechanical, Materials, and Aerospace Engineering; currently Graduate Student, Mechanical Engineering, Pennsylvania State University, University Park, PA 16802.

‡Member of the Technical Staff, Space Materials Laboratory; currently Graduate Student, Mechanical and Aerospace Engineering, University of California, Irvine, Irvine, CA 92697.

In the present study, a shock tube was employed to generate an SiH_4 oxidation and ignition database for the calibration of modern chemical kinetics models of silane combustion. Various H_2/O_2 and CH_4/O_2 mixtures with and without silane addition were tested. Provided in this paper are details on the experimental facility, measurement techniques, and procedures for testing these mixtures behind reflected shock waves. Typical data are presented in the form of species time histories, and the results of the experiments are given in terms of characteristic times as a function of test temperature.

Experiment

The key aspects of the experiments include the shock tube and related apparatus, the measurement techniques, and the procedure. Details are provided in the following sections.

Facility

All experiments were performed in the shock-tube facility at The Aerospace Corporation, as presented in Ref. 11. Although The Aerospace Corporation facility consists of two stainless-steel, helium-driven tubes, the lower tube was used exclusively in the present study. The driver section of the tube is 3.5 m (10 ft) long and has an internal diameter of 7.62 cm (3 in.). The driven section has a length of approximately 10.7 m (35 ft) with an internal diameter of 16.2 cm (6.38 in.). Lexan diaphragms of 0.25-mm (0.01-in.) thickness were utilized in tandem with a cutter located immediately downstream.

Ultimate pressures below 5×10^{-7} torr were obtained via overnight pumping with a 1000-l/s Leybold TMP1000C turbomolecular pump. Preexperiment ultimate pressures of 5×10^{-6} torr with a worst-case, combined leak and out-gassing rate of 1×10^{-4} torr/min were typical for most experiments. Fill pressures were monitored with three MKS Baratron model PDR-C-1B pressure transducers with 0–10, 0–100, and 0–1000 torr pressure ranges. Postshock test pressures were monitored by a Kistler 603B1 piezoelectric pressure transducer with a Kistler 5010 amplifier/signal conditioner box. Detection of the incident-shock speed was performed with five fast-response (<1-μs) PCB P113A pressure transducers and four Fluke model PM6666 time-interval counters. The pressure sensors were powered and amplified by a PCB 482A18 signal conditioner.

Test temperatures behind the reflected shock wave were determined from the incident-shock speed by the use of the standard one-dimensional shock-tube relations and the Sandia thermodynamic database.[12] The uncertainty of the reflected-shock temperature for the conditions herein has been determined previously and is approximately 5 K (Ref. 11). All data were recorded with a computer-based data acquisition system that consisted of a Pentium computer and a pair of CS512 computer oscilloscope boards from Gage Applied Sciences, giving a total of four channels at a speed of 5 MHz per channel with 12-bit resolution.

Diagnostics

Emission techniques were used to measure OH^*, CH^*, and SiH_4 time histories by focusing the emitted light through a 2-mm (or less) slit and onto a high-speed detector. The shock-tube windows were CaF_2, and the ports were located 1.6 cm from the endwall of the shock tube. Narrowband interference filters discriminated the emission from each species from background radiation. The overall time response of the emission diagnostics varied somewhat with the detector employed for each species, but, in general, was less than 5 μs.

For the silane concentration measurements, emission from the well-known ν_3 Si–H vibrational stretch mode was monitored through a filter centered at 4.7 ± 0.1 μm. Similar SiH_4 emission techniques have been utilized by others in shock-tube experiments, where the possibility of interference emission from coexisting Si_xH_x molecules was proven negligible over similar concentration ranges.[13] The infrared emission was measured with a 1-mm, LN_2-cooled Judson J10D InSb detector with a time response of less than 1 μs.

Chemiluminescence from the $A^2\Sigma^+$–$X^2\Pi$ transition of the excited hydroxyl radical OH^* was monitored by the use of a 310-nm filter with a 10-nm full width at half maximum (FWHM). To observe the low light levels, a detector that uses a Hamamatsu 1P21 photomultiplier tube (PMT) was employed. This PMT-based detector has been carefully designed and characterized to optimize the S/N while simultaneously minimizing the response time and ensuring linearity of the output signal.[14] The chemiluminescence from OH^* has been utilized in previous shock-tube experiments to determine when reaction occurs and, hence, has been a marker for ignition delay times in H_2/O_2 and CH_4/O_2 mixtures[15,16] and as an indicator of the presence of OH in flames.[17] Further details on the reaction rates of OH^* formation and quenching as well as its relation to OH in the ground state (and other species/reactions) is presented elsewhere.[18]

Ignition delay times for certain methane-based mixtures were determined when a filter with a 10-nm FWHM and the PMT detector described earlier were used to monitor the emission from excited CH molecules (CH^*) near 430 nm. The usefulness and accuracy of the use of CH^* as a marker for ignition has been demonstrated by Horning et al. in shock-tube experiments of heavy hydrocarbon ignition.[19]

Procedure

Several mixtures with and without silane were explored. Table 1 lists the mixture combinations reported in the present study. Each mixture was prepared in a stainless-steel mixing vessel by the use of the partial pressure method. The gases included ultrahigh purity (UHP) argon, UHP O_2, high-purity H_2, research-grade silane, and research-grade CH_4. Because silane is hypergolic at standard conditions, a special technique was developed to make premixed SiH_4/O_2/fuel/Ar mixtures in sufficient quantities to provide enough gas mixture for several shock-tube experiments.

Table 1 Mixtures for the shock-tube experiments, ϕ = fuel/oxidizer equivalence ratio

Mixture	%SiH_4	%O_2	%H_2	%CH_4	%Ar	ϕ
1	——	1.500	3.000	——	95.500	1.00
2	0.037	1.510	3.000	——	95.453	0.99
3	——	0.500	1.030	——	98.470	1.03
4	0.046	0.508	1.040	——	98.406	1.02
5	——	1.140	3.360	——	95.500	1.47
6	0.036	1.140	3.460	——	95.400	1.52
7	——	1.710	——	0.851	97.439	1.00
8	——	0.333	——	0.164	99.500	0.98
9	0.042	0.333	——	0.167	99.458	1.00

Because premature ignition occurred in initial attempts at making dilute mixtures of SiH_4/O_2 in argon in related experiments (despite the use of existing measurements of low-temperature silane ignition as a guide[20]), special care was taken when the mixtures containing silane were made. Premixture of the silane with argon and premixture of the oxygen in an argon-based mixture before their mutual introduction into the final mixing vessel was required to prevent spontaneous ignition of the silane in the mixing tank, even at low pressures and mixture ratios seemingly outside the flammability limits. A premixed tank containing 500-ppm SiH_4 in UHP argon was employed in all cases.

By the use of this premixing technique, mixtures with total pressures as high as 6 atm were made in the ratios presented in Table 1. To be certain the mixtures did not react before their use in the shock-tube experiments, windows were installed in the mixing tank, and a simple HeNe laser-extinction technique was applied to monitor whether or not silicon oxide powder was formed. The formation of powder was an indication that ignition had occurred in the vessel. No powder was detected during the preparation of mixtures containing SiH_4 in Table 1, and differences in the results between different mixtures with the same constituent mole fractions were not observed, which verified the repeatability of the process. No partial reaction within the mixing tank was observed. There was either no reaction for a successful mixture or complete oxidation of the silane in an unsuccessful mixture.

To minimize the temperature and pressure rise due to energy release and the gasdynamic effects associated with ignition in mixtures with relatively low levels of dilution, the mixtures in Table 1 were selected to maintain argon dilution levels greater than 95%. The specific levels of SiH_4 addition ($\approx$0.04%) were chosen because of the difficulties in preparing practical mixtures of silane and oxygen, as mentioned earlier, if the silane-to-oxygen ratio were too high. The resulting data set, described in detail in the following section, complements the earlier shock-tube data of McLain et al.[1] that, in contrast, utilized much lower levels of dilution ($\approx$85%) and much higher levels of SiH_4 concentration ($\approx$2%).

Results

Over 90 experiments were performed with the measurement techniques just described for the mixtures in Table 1. For all experiments, the average reflected-shock pressure was approximately 1 atm (with a range from 0.8 to 1.2 atm). The reflected-shock temperatures ranged from 1000 to 1760 K for the H_2-based mixtures and from 1690 to 2250 K for the CH_4-based mixtures. Presented hereafter are typical species time histories and characteristic-time plots for each mixture category. Table 2 lists the data for the entire set of experiments for future reference.

Hydrogen–Oxygen Mixtures

Ignition delay times of H_2/O_2 mixtures diluted in argon with and without silane addition were measured in the shock tube with OH^* chemiluminescence as the primary diagnostic. Baseline measurements of stoichiometric mixtures 1 and 3 (Table 1) were performed first, and a representative OH^* signal is presented in Fig. 1. The definition of ignition delay time in Fig. 1 was chosen because similar definitions tend to agree with existing ignition times based on pressure measurements and optical measurements involving other species.[21] The definition of τ_{p,OH^*} is also shown.

Note that the OH^* signal, although representative of ignition delay times, does not coincide exactly with the time history of ground state OH. The chemiluminescence signal is proportional instead to the excited OH molecules in the $A^2\Sigma^+$ state at a concentration that is several orders of magnitude less than the concentration of OH in the $X^2\Pi$ state. The resulting differences are best demonstrated by the use of chemical kinetics modeling with a detailed mechanism (such

Table 2 Experimental results for all mixtures (specific mixtures provided in Table 1)

T, K	p, atm	τ_p, μs	τ_{ign}, μs
	Mixture 1		
1423	1.07	196	133
1244	1.15	335	258
1173	1.13	477	381
1340	1.14	244	175
1149	1.2	550	450
1200	1.15	421	325
1096	1.14	643	512
1148	1.36	425	344
1048	1.26	873	721
1173	1.3	391	315
1009	1.19	1184	1055
1026	1.12	952	812
1130	1.24	492	406
1182	1.04	470	370
1430	1.06	168	109
1275	1.03	319	231
1399	1.14	195	135
1203	1.23	354	290
1335	1.3	191	148
1219	1.17	359	300
1240	1.09	340	262
1364	1.18	193	143
1133	1.23	514	431
1351	1.21	191	158
	Mixture 2		
1090	1.13	346	243
1144	1.17	256	174
1179	1.17	222	146
1127	1.3	267	177
1254	1.22	151	91
1242	1.13	170	105
1335	1.11	124	68
1401	1.1	102	52
1057	1.28	432	308
	Mixture 3		
1389	1.16	526	346
1181	1.14	1277	979
1544	0.98	358	207
1302	1.19	699	462
1442	1.05	444	269
1270	1.22	805	601
1311	1.13	629	443
1432	1.13	415	250
1752	0.95	249	93
	Mixture 4		
1565	1.21	135	73
1187	1.29	608	382
1075	1.2	1276	820
1208	1.19	573	368
1211	1.06	666	397
1408	1.19	267	154
1124	1.29	865	583
1435	1.13	226	133
	Mixture 5		
1225	1.14	367	274
1111	1.2	697	568
1511	1.2	165	120
1305	1.11	277	201
	Mixture 6		
1301	1.26	138	83
1131	1.25	299	230
1435	1.12	106	51
1358	1.18	125	63
1184	1.21	268	183
1229	1.2	225	145
	Mixture 7		
1836	0.8	716	653
1687	0.93	——	1899
1814	0.92	798	727
1807	0.9	781	724
1774	0.98	1032	970
2008	0.81	252	210
1957	0.88	336	284
1836	0.88	648	581
1844	0.86	——	625[a]
	Mixture 8		
2187	0.85	——	205[a]
1877	0.9	1456[a]	1296[a]
1940	0.84	904[a]	796[a]
2052	0.85	502[a]	421[a]
2242	0.88	196[a]	141[a]
2150	0.77	298[a]	229[a]
2230	0.81	218[a]	160[a]
1948	0.88	817[a]	706[a]
1870	0.9	1394[a]	1266[a]
1944	0.86	906[a]	799[a]
2004	0.86	611[a]	521[a]
2213	0.93	216[a]	162[a]
2109	0.81	337	202
2080	0.85	449	289
1972	0.87	877	677
1874	0.88	1497	1290
2214	0.73	214	105
	Mixture 9		
1911	0.86	385[a]	272[a]
1970	0.97	298[a]	201[a]
1818	0.94	533[a]	401[a]
1691	0.06	1150[a]	915[a]
1962	0.9	326[a]	227[a]
2086	0.91	196[a]	125[a]
2132	0.87	193[a]	116[a]

[a]Using CH chemiluminesence (all others from OH).

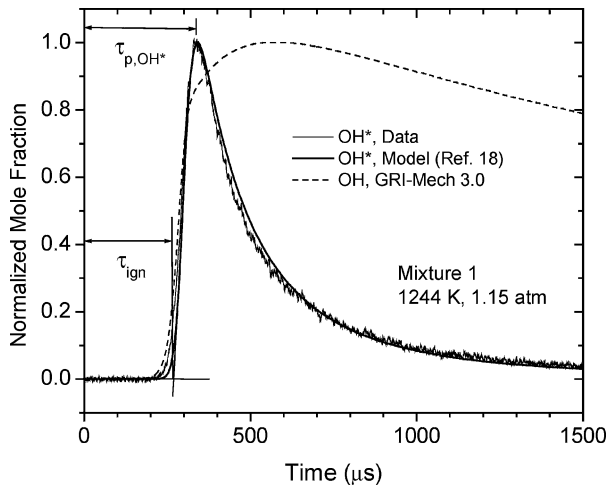

Fig. 1 Measured and calculated OH* and OH time histories for H_2/O_2 mixture 1, showing definition of characteristic times.

as the GRI-Mech 3.0 mechanism of Smith, G. P., Golden, D. M., Frenklach, M., Moriarty, M. W., Eiteneer, B., Goldenberg, M., Bowman, C. T., Hanson, R. K., Song, S., Gardiner, W. C., Lissianski, V. V., and Qin, Z., URL: http://www.me.berkeley.edu/gri_mech/. [cited 10 February 2004]) having additional reactions for OH* chemistry.[18] A typical result given by the CHEMKIN software[22] is also presented in Fig. 1 for the conditions of a reflected-shock experiment at 1244 K, 1.15 atm by the use of mixture 1. In general, the initial rise of OH* and OH agree favorably (with OH leading OH* slightly), hence leading to similar τ_{ign} values as defined herein. However, τ_{p,OH^*} is noticeably shorter than $\tau_{p,OH}$, and the ground state OH molecules last longer than the excited molecules. Hence, care should be exercised when OH behavior is inferrred from OH* signals. Further comparisons between OH and OH* chemistry and related chemical kinetics calculations are provided elsewhere.[18]

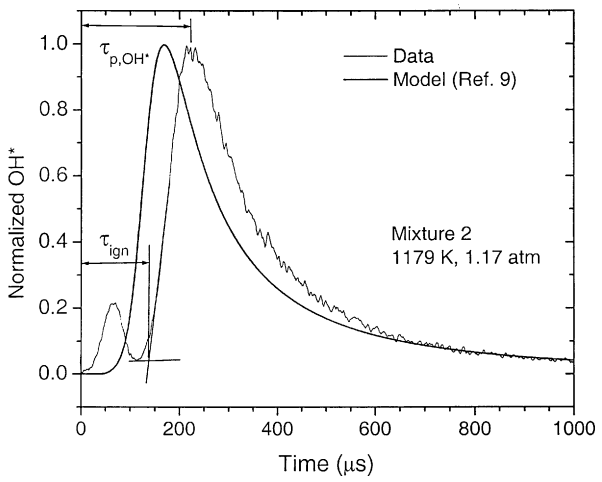

Fig. 2 Measured and calculated OH* profiles for $SiH_4/H_2/O_2$ mixture 2, showing interference emission peak near time zero and the primary OH* peak due to H_2/O_2 ignition; model from Miller et al.,[9] modified for OH* chemistry per Kalitan and Petersen.[27]

When silane was added to a H_2/O_2 mixture, the OH* signal displayed a double-peak structure, as shown in Fig. 2. The first peak shortly after reflected-shock arrival was only observed when SiH_4 was present, and it is believed to be due to the rapid thermal decomposition of the silane; the second peak is from the ignition of the bulk hydrogen/oxygen within the mixture. The source of the first peak in the signal does not represent OH* but, rather, is thought to be interference emission from species present during the initial decomposition of the SiH_4. As shown by Park and Fujiwara[23] in shock-heated SiH_4/Ar mixtures, silicon-containing species such as Si_2 and SiH have rather strong, broadband emission features stretching from the ultraviolet (as low as 250 nm) to the visible (440 nm and higher). The authors' hypothesis that the first peak in Fig. 2 is not OH* was confirmed both analytically and experimentally, as follows.

By the use of kinetics modeling, it was shown that OH* is expected to have only a single peak for mixtures and conditions corresponding to the experiments herein. The results of a SiH_4 oxidation kinetics model calculation, by the use of the Miller et al. mechanism,[9] does not predict the smaller first peak for OH* (Fig. 2). Additional experiments by the authors using SiH_4/Ar mixtures (that is, no oxygen present) in conjunction with the OH* optical setup displayed similar emission peaks in the 310-nm wavelength range.

Additionally, it is well known that silane decomposes quite readily at temperatures as low as 1200 K. Parallel experiments by the authors have demonstrated that SiH_4 decomposition occurs within the timescales represented by the interference peak in the OH* emission signals at the time immediately after reflected-shock arrival.[24] A typical silane decomposition measurement is shown in Fig. 3 with and without the presence of O_2, where the measured SiH_4 concentration was obtained from the SiH_4 infrared- (IR)-emission diagnostic described earlier. Because of the time lag of the optical setup at the instant of reflected-shock arrival, the SiH_4 signals in Fig. 3 are both normalized to the concentrations at some time t^* after time zero, where $t^* = 25$ μs for the cases shown.

Because silane decomposes so readily, the possibility of silane pyrolysis and/or oxidation behind the incident wave before the arrival of the reflected shock wave is a potential concern. This possibility was checked with a typical SiH_4 oxidation kinetics model[9] to estimate the level of silane combustion, if any, at the extreme postincident-shock conditions of this study. For a reflected-shock temperature of 1400 K and pressure of 1.1 atm, the conditions behind the corresponding incident wave would be around 700 K and 0.3 atm and would last approximately 45 μs before reflected-shock arrival. Under these conditions, no perceptible SiH_4 removal was observed.

Care should also be practiced when τ_{p,OH^*} measurements are used to represent ignition-delay times for the H_2/O_2 mixtures herein. A comparison between the two characteristic times, τ_{ign} and τ_{p,OH^*}, is presented in Fig. 4 as a function of inverse temperature for H_2/O_2 ignition without silane addition. The two characteristic times differ by as much as a factor of 2–3 at higher temperatures. Also, the activation energies for the ignition times, given in Table 3, are slightly higher than the activation energies of the peak OH* times. Given the uncertainties in obtaining characteristic times from the species profiles (per Fig. 1), the overall uncertainty in any τ_{ign} or τ_p measurement is nonetheless no greater than 10% of the specified value.

Table 3 Parameters for characteristic times, where $\tau = C \exp(E/RT)$

	τ_p, μs		τ_{ign}, μs	
Mixture	C	E, kcal/mol	C	E, kcal/mol
1[a]	1.62	13.4	0.72	14.7
2	1.45	11.7	0.25	14.8
3	8.08	11.6	0.87	16.4
4	1.3	14.7	0.48	15.9
5	2.97	11.9	1.55	12.8
6	1.42	12.1	0.12	17.2
7[b]	6.76×10^{-3}	42.0	2.02×10^{-3}	46.1
8[b]	1.16×10^{-2}	43.4	2.64×10^{-3}	48.6
9[b]	0.17	29.3	3.80×10^{-2}	33.7

[a]Adjusted to a pressure of 1 atm. [b]Based on CH* measurements.

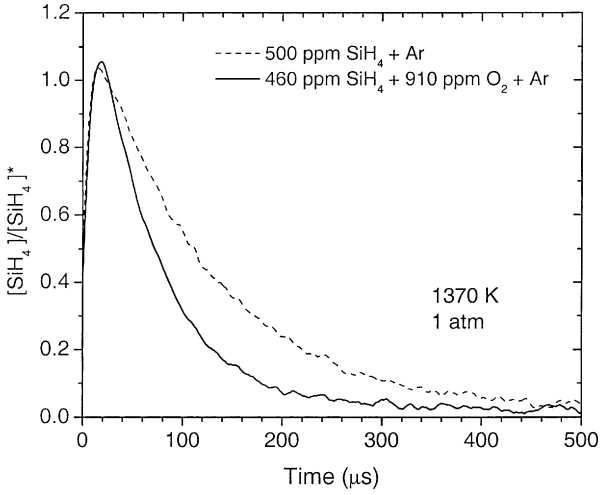

Fig. 3 Normalized SiH_4 concentration for two mixtures: 500-ppm SiH_4 and no O_2 and 460-ppm SiH_4 and O_2 at $\phi = 1.17$.

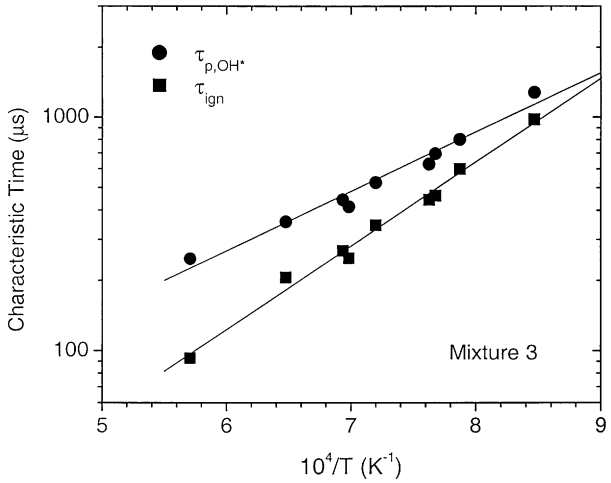

Fig. 4 Comparison between characteristic times τ_{ign} and τ_{p,OH^*} for H_2/O_2 mixture 3; note differences in magnitude and slope, particularly at higher temperatures.

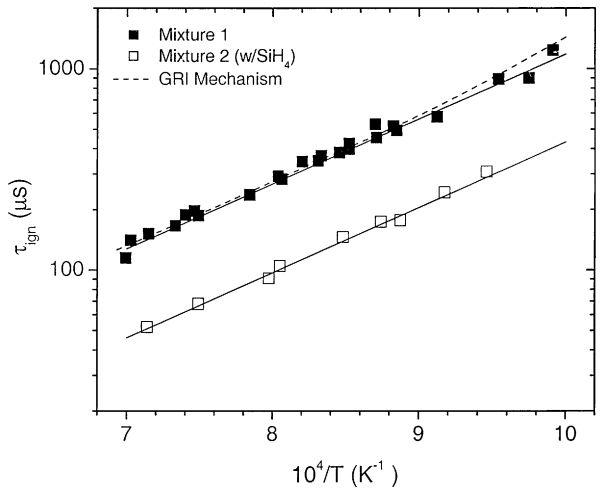

a) Ignition-delay times

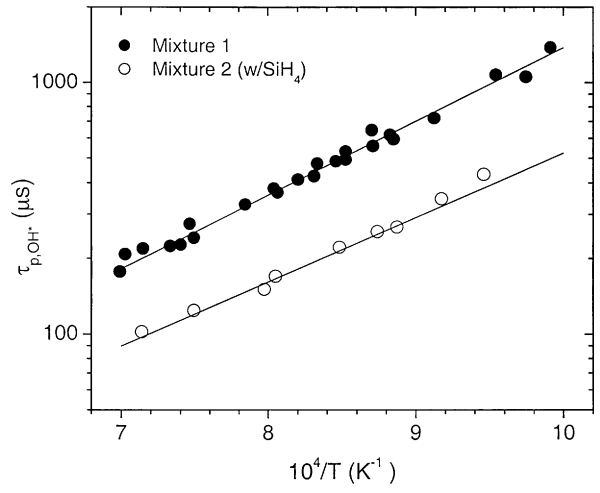

b) Time-to-peak OH* formation

Fig. 5 Characteristic times for the high-concentration stoichiometric H_2/O_2 mixtures with and without SiH_4 (mixtures 1 and 2, Table 1).

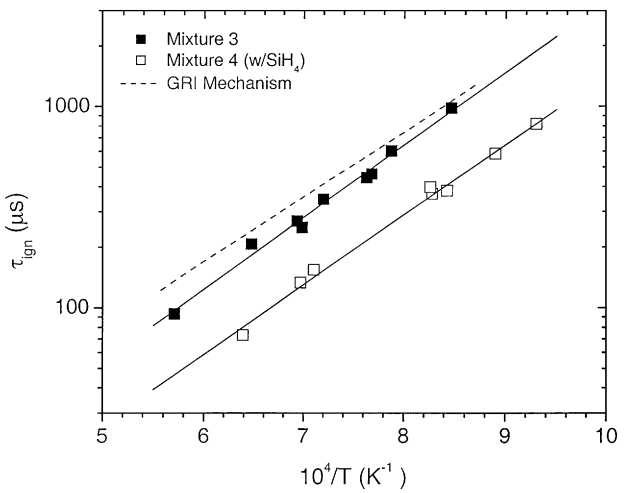

a) Ignition-delay times

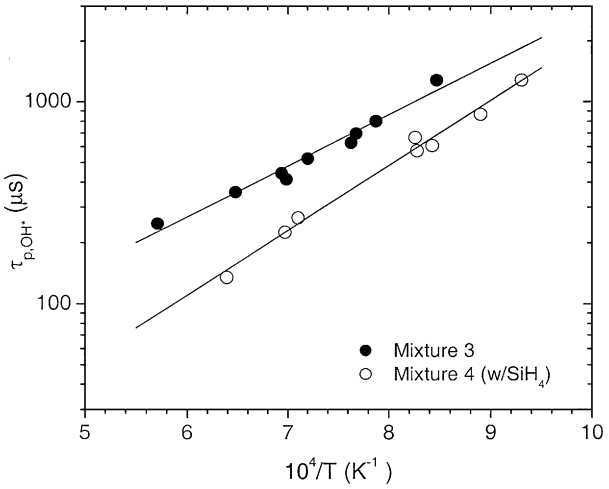

b) Time-to-peak OH* formation

Fig. 6 Characteristic times for the low-concentration stoichiometric H_2/O_2 mixtures with and without SiH_4 (mixtures 3 and 4, Table 1).

For either characteristic time, the present experiments clearly demonstrate the accelerating effect that silane has on H_2/O_2 ignition. Figure 5a compares the ignition-delay times for the higher-concentration, stoichiometric mixtures 1 and 2 (Table 1), and Fig. 5b compares the corresponding time to peak OH* for the same experiments. For both characteristic times, the presence of SiH_4 results in lower values, typically a factor of two or more for most temperatures.

The current results are significant in that the silane concentration in mixture 2 is only about 1% of the total fuel concentration. When plotted vs $1/T$, the logarithm of the characteristic times produces a straight line, as seen in Fig. 5. Note that the data in Fig. 5 for mixture 1 were adjusted slightly to conform to a common pressure of 1 atm by the use of the pressure dependencies described hereafter; the raw data are provided in Table 2.

Also shown in Fig. 5a is the excellent agreement between the ignition-time values for mixture 1 (without SiH_4) and the predictions of an established hydrogen–oxidation kinetics model. The kinetics model used was the H_2/O_2 subset of the GRI–Mech. 3.0 methane oxidation mechanism (Smith, G. P., Golden, D. M., Frenklach, M., Moriarty, M. W., Eiteneer, B., Goldenberg, M., Bowman, C. T., Hanson, R. K., Song, S., Gardiner, W. C., Lissianski, V. V., and Qin, Z., URL: http://www.me.berkeley.edu/gri_mech/. [cited 10 February 2004]). The calculations were performed using CHEMKIN.[22]

Similar results are seen in the lower-concentration, stoichiometric mixtures 3 and 4 (Table 1) in Figs. 6a and 6b. The acceleration of the reaction is evident in the decreased τ_{ign} and τ_p values seen in Fig. 6.

Experiments were also performed by the use of the fuel-rich H_2/O_2 mixture with a fuel-to-oxidizer equivalence ratio near 1.5, that is, mixtures 5 and 6 (Table 1). Figure 7 presents the ignition-delay and time-to-peak OH* results as a function of inverse temperature. A factor-of-two decrease in both characteristic times for the fuel-rich mixtures was observed (Fig. 7).

The time-to-peak OH* and other characteristic times in this study can be represented by the relation

$$\tau = C \exp(E/RT) \tag{1}$$

where τ is the characteristic time in microseconds, C is a constant, E is an activation energy in kilocalories per mole, R is the universal gas constant, and T is the temperature in Kelvins. Note that for each mixture, most experiments were performed at pressures near 1 atm, so that a pressure dependence was not needed to fit the data with Eq. (1) (except for mixture 1, as mentioned earlier). The results are given in Table 3 for each mixture. The H_2/O_2 activation energies for the $\phi = 1$ mixtures range from 14.5 to 16.4 kcal/mol for τ_{ign} and from 11.6 to 14.7 kcal/mol for τ_p. In general, the activation energies for the ignition times were about 2 kcal/mol higher than their time-to-peak OH* counterparts, and the presence of SiH_4 resulted in little, if any, change in E for either characteristic time.

To determine the concentration dependence on ignition delay, a least-squares fit correlation was performed for τ_{ign} and τ_{p,OH^*} for all mixtures containing H_2/O_2/Ar. In general, ignition delay data can

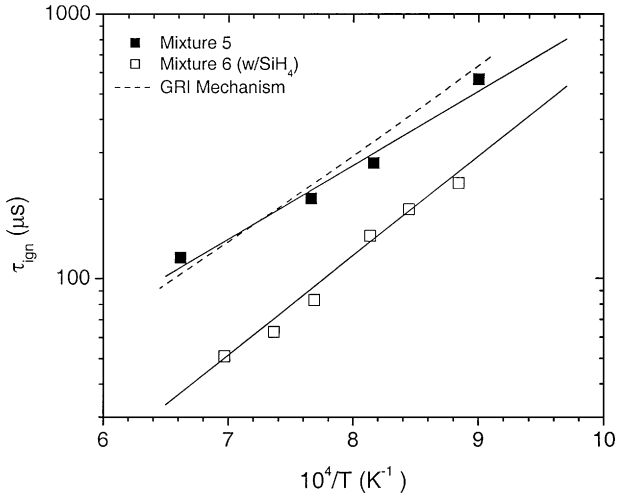

a) Ignition-delay times

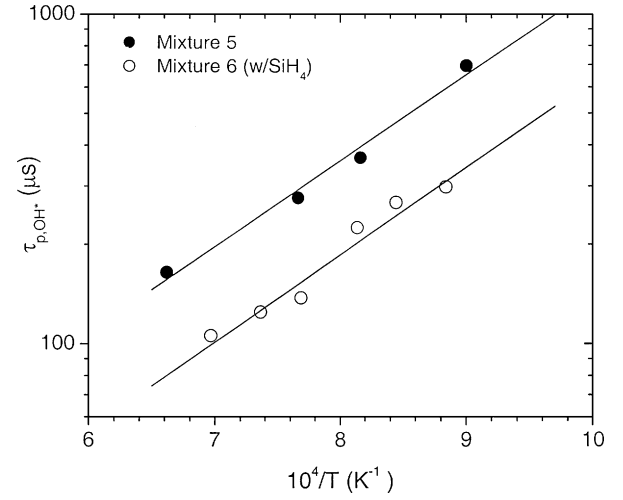

b) Time-to-peak OH* formation

Fig. 7 Characteristic times for the fuel-rich H_2/O_2 mixtures with and without SiH_4 (mixtures 5 and 6, Table 1).

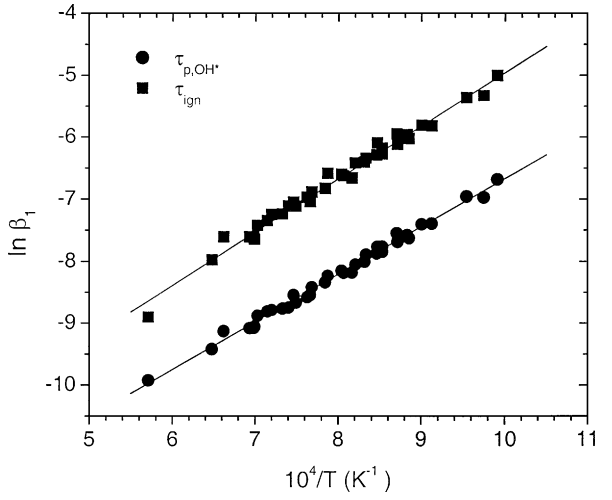

a) H_2/O_2/Ar mixtures, β_1 as defined in Eq. (5)

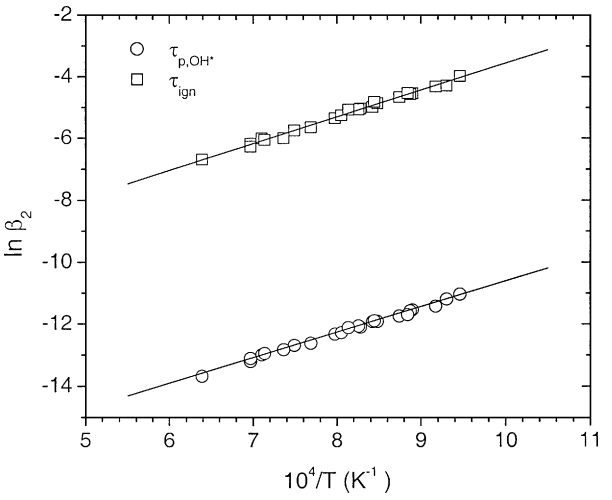

b) $SiH_4/H_2/O_2$/Ar mixtures, β_2 as defined in Eq. (8)

Fig. 8 Overall ignition-delay correlations for H_2/O_2 mixtures with and without silane.

be correlated into an equation of the form

$$\tau = \mathrm{A[FUEL]}^a[\mathrm{O_2}]^b[\mathrm{SiH_4}]^c \exp(\mathrm{E/RT}) \quad (2)$$

It was determined that the ignition delay for the onset of OH* emission for the hydrogen/oxygen mixtures varied as

$$\tau_{\mathrm{ign}} = 1.34 \times 10^{-6}[\mathrm{H_2}]^{-0.24}[\mathrm{O_2}]^{-0.55} \exp(17.0/\mathrm{RT}) \quad (3)$$

where τ_{ign} is in microseconds, the activation energy of 17.0 is in kilocalories per mole, the temperature T is in Kelvins, and the concentrations are in moles per cubic centimeter. Equation (3) has a statistical coefficient of multiple regression, or R^2, value of 0.974. Also, the overall pressure dependence of the H_2/O_2 ignition times is seen in the overall concentration exponent of −0.79.

The characteristic times based on the peak of the OH* emission are described by the following equation:

$$\tau_{p,\mathrm{OH^*}} = 5.72 \times 10^{-7}[\mathrm{H_2}]^{-0.32}[\mathrm{O_2}]^{-0.59} \exp(15.3/\mathrm{RT}) \quad (4)$$

This equation has $R^2 = 0.985$ and an overall pressure-dependent exponent of −0.91. All of the H_2/O_2/Ar data are plotted in Fig. 8a, where, in general,

$$\beta_1 = \tau[\mathrm{H_2}]^{-a}[\mathrm{O_2}]^{-b} \quad (5)$$

and the correlation is shown to be accurate.

The process was repeated for all $H_2/O_2/SiH_4$/Ar mixtures, and the ignition delays can be expressed as

$$\tau_{\mathrm{ign}} = 2.40 \times 10^{-7}[\mathrm{H_2}]^{0.67}[\mathrm{O_2}]^{-1.65}[\mathrm{SiH_4}]^{0.17} \exp(18.4/\mathrm{RT}) \quad (6)$$

$$\tau_{p,\mathrm{OH^*}} = 9.19 \times 10^{-10}[\mathrm{H_2}]^{0.59}[\mathrm{O_2}]^{-1.62}[\mathrm{SiH_4}]^{-0.13} \exp(17.1/\mathrm{RT}) \quad (7)$$

Both correlations for the $H_2/O_2/SiH_4$/Ar mixtures have $R^2 = 0.99$, as shown in Fig. 8b, where

$$\beta_2 = \tau[\mathrm{H_2}]^{-a}[\mathrm{O_2}]^{-b}[\mathrm{SiH_4}]^{-c} \quad (8)$$

As expected from the results of the individual correlations (Table 3), the silane had very little effect on the overall activation energy for either characteristic time. In addition, there was negligible dependence on argon for all hydrogen mixtures studied in this experiment.

Methane–Oxygen Mixtures

Reflected-shock ignition of the CH_4/O_2/Ar and $CH_4/O_2/SiH_4$/Ar mixtures in Table 1 were measured over a range of temperatures from 1690 to 2250 K. At the extreme temperature limit, the hottest condition behind the incident shock wave was about 1100 K, and at this condition less than 1% of the silane reacted before reflected-shock arrival per the results of a chemical kinetics calculation using the Miller et al. mechanism[9] (but without CH_4). Reaction progress during the methane experiments was monitored by the use of CH*

and OH* chemiluminescence as described earlier. Sample time histories of OH* and CH* from the experiments are given in Figs. 9–11. The definition of the two characteristic times are shown for OH* in Fig. 9 and for CH* in Fig. 10.

As observed in the OH* measurements with the H_2/O_2 mixtures, the CH* profiles showed an earlier peak when SiH_4 was added to the methane-based mixtures. Through exploratory experiments, the authors concluded that the first peak immediately after reflected-shock arrival (as in Fig. 11) is not due to CH* chemiluminescence near 430 nm but is instead due to broadband interference emission from Si_2, SiH, or similar species present during the decomposition of the silane, as discussed earlier.

For both measured species (CH* and OH*), the profiles as seen in Figs. 9–11 are much narrower (100–200 μs) than corresponding profiles observed in the H_2/O_2 measurements. The resulting usefulness of CH* emission measurements as a marker in hydrocarbon ignition has been demonstrated previously.[19] When τ_{ign} measurements derived from CH emission are compared to τ_{p,CH^*} measurements, as in Fig. 12, the agreement between the two is better than in similar comparisons using OH* measurements in H_2/O_2 mixtures, for example, Fig. 4. Table 2 lists the characteristic times for the methane-based mixtures 7–9 defined in Table 1.

When silane was added to the stoichiometric CH_4/O_2 mixtures, a marked reduction in ignition-delay time was observed. Figure 13a shows the results in terms of ignition-delay time, and Fig. 13b shows the results for peak CH* formation. Also displayed in Fig. 13a is a

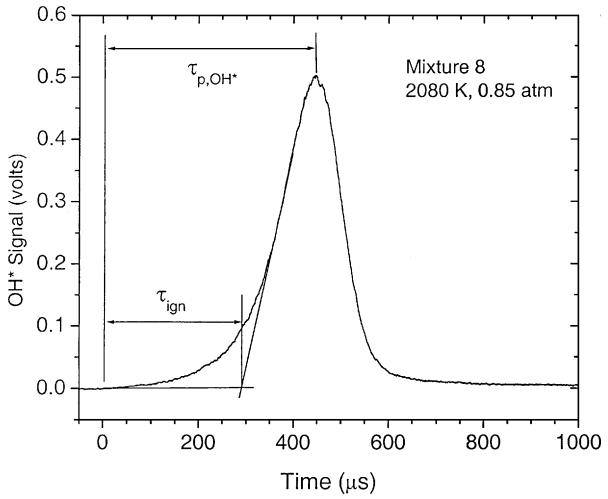

Fig. 9 Typical OH* emission signal for CH_4/O_2/Ar mixture 8 showing characteristic times.

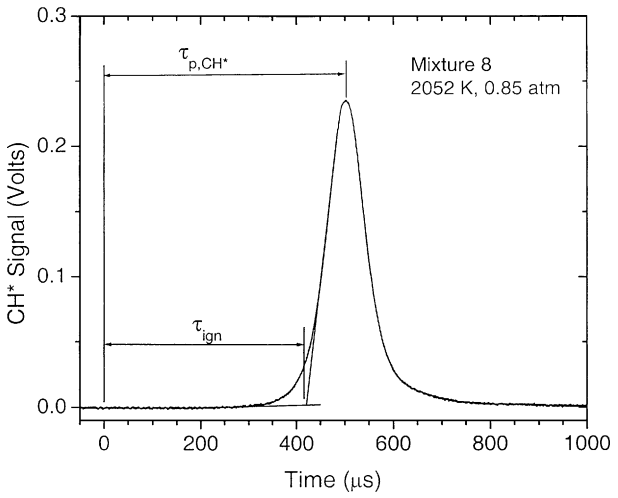

Fig. 10 Typical CH* emission signal for CH_4/O_2/Ar mixture 8 showing characteristic times.

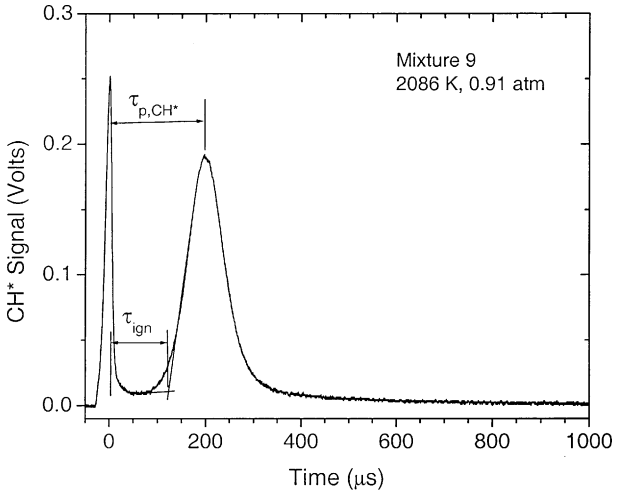

Fig. 11 Typical CH* emission signal for $SiH_4/CH_4/O_2$/Ar mixture 9, showing characteristic times and interference peak near time of reflected-shock arrival.

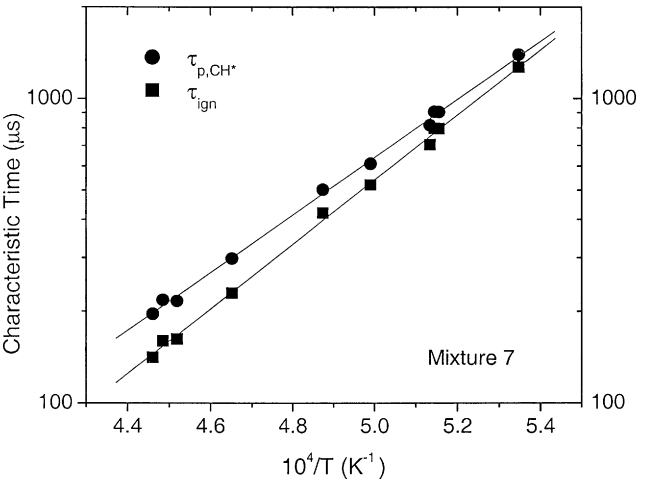

Fig. 12 Comparison between characteristic times τ_{ign} and τ_{p,CH^*} for CH_4/O_2/Ar mixture 7.

comparison with the methane τ_{ign} correlation from Petersen et al.,[25] which shows good agreement between the established correlation and the present data for the CH_4/O_2/Ar mixture.

Whereas the τ_{ign} slopes for the mixtures without SiH_4 addition (46.1 and 48.6 kcal/mol) are similar to the activation energies observed in the well-studied ignition of methane,[26] a 30% reduction in ignition activation energy is seen when SiH_4 is added (33.7 kcal/mol), as shown in Table 3 and Fig. 13. Also evident in the methane-ignition data is the good agreement in the peak times derived from OH* and CH* formation (Fig. 13b).

In contrast, there is poor agreement between τ_{ign} obtained from OH* and τ_{ign} obtained from CH* at higher temperatures (Fig. 13a). By comparison of a typical OH* profile (Fig. 9) with a CH* profile (Fig. 10) at similar, high temperatures, it can be seen that the OH* exhibits a more gradual rise that begins sooner than the CH* formation, leading to the earlier τ_{ign}. The authors recommend caution when working with characteristic time data taken from different species diagnostics, particularly when results from kinetics calculations are interpreted and they are compared to shock-tube data.

Discussion

Additional insight can be gained by comparison of the data herein to the results of the most recent chemical kinetics models of silane oxidation and to the one earlier shock-tube study of $SiH_4/H_2/O_2$ oxidation. As mentioned, several chemical kinetics models of silane oxidation exist in the literature, for example, those of Golovitchev

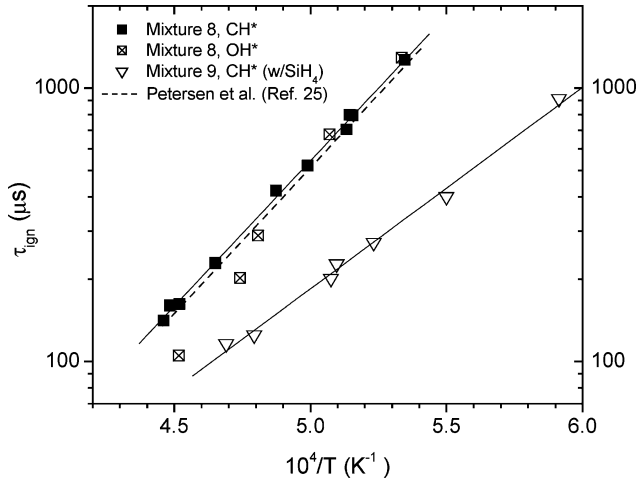

a) Ignition-delay times

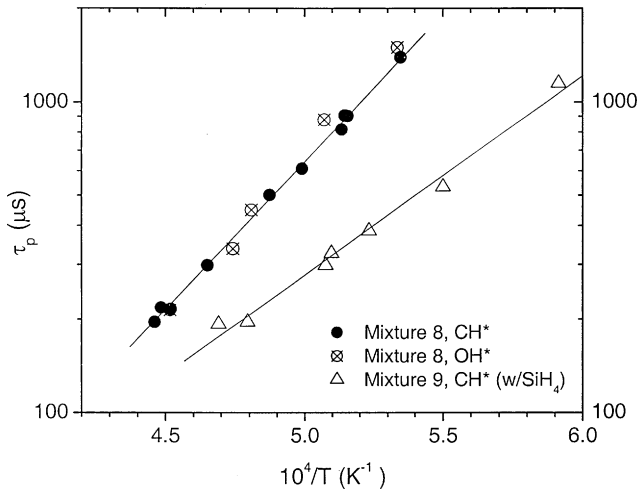

b) Time-to-peak OH* formation

Fig. 13 Characteristic times for the stoichiometric CH_4/O_2 mixtures with and without SiH_4 (mixtures 8 and 9, Table 1).

and Bruno,[8] Miller et al.,[9] and Babushok et al.,[10] among others. A detailed comparison of several mechanisms with the present data is provided elsewhere,[27] although a few results are included in this paper for completeness. For example, the Miller et al.[9] mechanism was used to generate the analytical OH* profile in Fig. 2. As Fig. 2 indicates, the SiH_4 kinetics model captures the basic shape of the OH* formation and depletion. Nonetheless, even this kinetics model does not reproduce the entire range of data as well as implied in Fig. 2, nor do most of the other mechanisms.[27]

The models can nonetheless be used to model the basic trends witnessed herein, namely, the acceleration of H_2/O_2 ignition when SiH_4 is added. The effect is even more pronounced when a model is used to extend the H_2/O_2 ignition results into the well-known second explosion limit at lower temperatures (and higher pressures).[21] Figure 14 shows model calculations along with the extent of the higher temperature data for mixtures 1 and 2, without and with silane. Note again that the slope of the τ_{ign} data changes very little between the two mixtures at higher temperatures, which implies similar chain-branching kinetics through the propagation of H, OH, and O radicals, although not necessarily through the same dominant reaction steps. The Miller et al.[9] kinetics model also shows that the ignition activation energy extends into the lower temperature regime.

It is well known that when the H_2/O_2 mixture without silane is at lower temperatures (<1000 K), the chain termination through the $H + O_2 = HO_2$ reaction severely retards the overall reactivity of the combustion process. The presence of silane seems to curtail the HO_2 formation path, encouraging instead chain branching through the H,

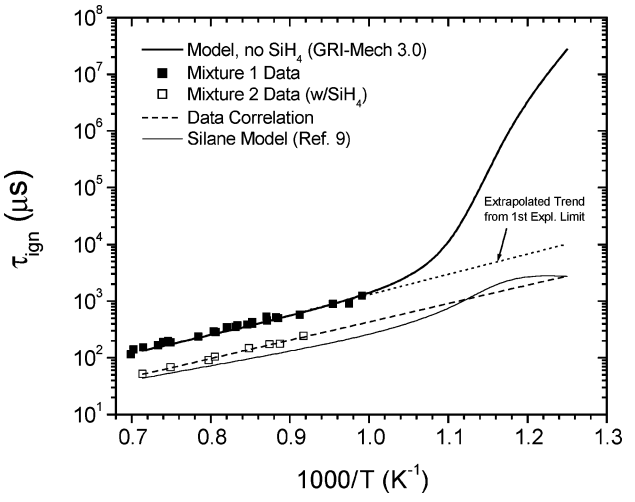

Fig. 14 Effect of silane addition on H_2/O_2 ignition kinetics; characteristics of the second explosion limit at low temperatures are represented by the GRI–Mech 3.0 mechanism (Smith, G. P., Golden, D. M., Frenklach, M., Moriarty, M. W., Eiteneer, B., Goldenberg, M., Bowman, C. T., Hanson, R. K., Song, S., Gardiner, W. C., Lissianski, V. V., and Qin, Z., URL: http://www.me.berkeley.edu/gri_mech/.) when no SiH_4 is present and the Miller et al. mechanism[9] when SiH_4 is added.

OH, and O radicals and effectively extending the first explosion limit to lower temperatures. The net effect is that the presence of silane at lower temperatures can potentially decrease the ignition delay time by several orders of magnitude if the results of the kinetics model are correct.

Although the experimental results of McLain et al.[1] cannot be directly compared to the shock-tube results herein because of the extreme differences in mixture composition, the trends predicted by both can be compared through the use of kinetics modeling. Figure 15 shows the results of the earlier experiment (including SiH_4) in comparison with the numerical results of the GRI–Mech 3.0 mechanism (Smith, G. P., Golden, D. M., Frenklach, M., Moriarty, M. W., Eiteneer, B., Goldenberg, M., Bowman, C. T., Hanson, R. K., Song, S., Gardiner, W. C., Lissianski, V. V., and Qin, Z., URL: http://www.me.berkeley.edu/gri_mech/.) for an equivalent mixture without silane over the same temperature range as the experiments. (McLain et al. did not test H_2/O_2 mixtures without silane, most likely because the ignition-delay times would have been much too long for a typical shock-tube experiment.[1]) Figure 15a presents the result for McLain et al., mixture 1, and Fig. 15b presents the results for McLain et al., mixture 2.

The results in Fig. 15 corroborate the present finding that the activation energy is almost unaffected by the addition of silane at higher temperatures, but that the addition of silane greatly speeds up the ignition process. Even more evident is the fact that the measurements actually indicate that the activation energy trend indeed continues into the lower temperature regime, completely eliminating the chain-termination kinetics evident in the mixture without SiH_4. Hence, the data of McLain et al.,[1] although at much different temperatures and mixture compositions than those herein, tend to confirm the findings of this paper: 1) SiH_4 greatly reduces the ignition time of H_2/O_2 mixtures. 2) SiH_4 erases the second explosion limit behavior expected of H_2/O_2 mixtures at lower temperatures. Further insight into the detailed kinetics is provided in Ref. 27.

Note that even less kinetics information is available for methane and other hydrocarbons with silane addition. One exception is the model presented by Takahashi et al.[4] for C_2H_2, C_2H_4, and C_2H_6 combustion in the presence of silane. In their work, interactions between carbon compounds and silicon compounds were ignored, under the assumption that the hydrocarbons interacted with the silicon-containing molecules solely by the exchange of radical species such as H, OH, and O. Further exploration into the kinetics of hydrocarbon oxidation in the presence of silane is certainly needed, but is beyond the scope of this paper.

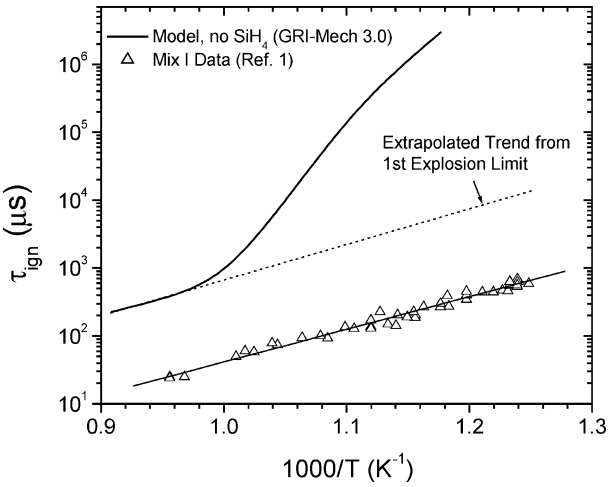

a) McLain et al. mixture 1 (2% SiH_4 + 8% H_2 + 4.01% O_2 + 85.99% N_2)

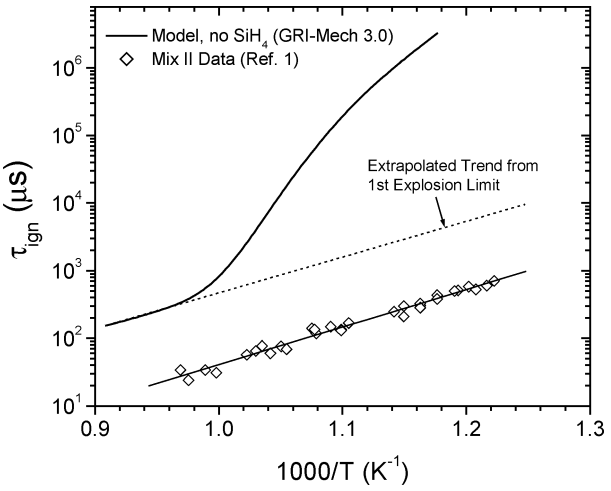

b) McLain et al. mixture 2 (1.68% SiH_4 + 6.72% H_2 + 6.74% O_2 + 84.86% N_2)

Fig. 15 Silane acceleration of H_2/O_2 ignition inferred from the McLain et al. shock-tube data[1] by comparison to the GRI–Mech 3.0 H_2/O_2 submechanism (Smith, G. P., Golden, D. M., Frenklach, M., Moriarty, M. W., Eiteneer, B., Goldenberg, M., Bowman, C. T., Hanson, R. K., Song, S., Gardiner, W. C., Lissianski, V. V., and Qin, Z., URL: http://www.me.berkeley.edu/gri_mech/.).

Summary

Although silane oxidation and ignition are important in applications such as aerospace propulsion and materials processing, few fundamental data exist at elevated temperatures. In the present study, experiments were performed behind reflected shock waves over a range of temperatures from 1000 to 2250 K, using several argon-diluted mixtures with and without SiH_4. The mixtures included $H_2/O_2/Ar$, $H_2/O_2/SiH_4/Ar$, $CH_4/O_2/Ar$, and $CH_4/O_2/SiH_4/Ar$. Reaction progress was followed by the use of a combination of OH^* and CH^* chemiluminescence and SiH_4 emission. Characteristic times were used to display the data, including ignition-delay times and time-to-peak formation of CH^* and/or OH^*.

For hydrogen mixtures, the data were correlated to form a general equation that describes the ignition-delay dependence on concentration as well as temperature. On comparison of the ignition behavior of mixtures with and without SiH_4, it was observed that the presence of SiH_4 reduced the ignition-delay time by as much as a factor of two or more, even for relatively small concentrations of silane (4% or less of the primary fuel volume). Limited chemical kinetics modeling was also performed in support of the data reduction and interpretation. The models, in conjunction with the data, indicate that silane has little effect on the ignition-delay time activation energy of hydrogen-based mixtures and blocks the tendency of such mixtures to exhibit the shift in kinetics from a chain-branching process in the first explosion limit at higher temperatures to a chain-termination process in the second explosion limit at lower temperatures. Significant reductions in ignition-delay time were also observed for the methane-based mixture when silane was added. The characteristic times, along with the species concentration histories, can be used to calibrate detailed chemical kinetics models of silane-related oxidation and to formulate a better understanding of silane oxidation and related ignition chemistry.

Acknowledgments

This work was supported by The Aerospace Corporation and The Air Force Space and Missile Systems Center under Contract F04701-00-C-0009. The assistance of Carrol Gardner and Mark Crofton in the laboratory is appreciated.

References

[1]McLain, A. G., Jachimowski, C. J., and Rogers, R. C., "Ignition of SiH_4–H_2–O_2–N_2 Behind Reflected Shock Waves," NASA TP 2114, 1983.

[2]Jachimowski, C. J., and McLain, A. G., "A Chemical Kinetic Mechanism for the Ignition of Silane/Hydrogen Mixtures," NASA TP 2129, 1983.

[3]Lewis, M. J., and Chang, J. S., "Joint Jet-A/Silane/Hydrogen Reaction Mechanism," *Journal of Propulsion and Power*, Vol. 16, No. 2, 2000, pp. 365–367.

[4]Takahashi, T., Hagiwara, K., Egashira, Y., and Komiyama, H., "The Effect of Gas-Phase Additives C_2H_4, C_2H_6, and C_2H_2 on SiH_4/O_2 Chemical Vapor Deposition," *Journal of the Electrochemical Society*, Vol. 143, No. 4, 1996, pp. 1355–1361.

[5]Wooldridge, M. A., "Gas-Phase Combustion Synthesis of Particles," *Progress in Energy and Combustion Science*, Vol. 24, No. 1, 1998, pp. 63–87.

[6]Britten, J. A., Tong, J., and Westbrook, C. K., "A Numerical Study of Silane Combustion," *Proceedings of the Combustion Institute*, Vol. 23, 1990, pp. 195–202.

[7]Koda, S., "Kinetic Aspects of Oxidation and Combustion of Silane and Related Compounds," *Progress in Energy and Combustion Science*, Vol. 18, No. 6, 1992, pp. 513–528.

[8]Golovitchev, V. I., and Bruno, C., "Numerical Study of the Ignition of Silane/Hydrogen Mixtures," *Journal of Propulsion and Power*, Vol. 15, No. 1, 1998, pp. 92–96.

[9]Miller, T. A., Wooldridge, M. S., and Bozzelli, J. W., "Computational Modeling of Silane Combustion," *Proceedings from the Third Joint Meeting of the U.S. Sections of the Combustion Institute*, Combustion Inst., Pittsburgh, PA, 2003.

[10]Babushok, V. I., Tsang, W., Burgess, D. R., and Zachariah, M. R., "Numerical Study of Low- and High-Temperature Silane Combustion," *Proceedings of the Combustion Institute*, Vol. 27, 1998, pp. 2431–2439.

[11]Petersen, E., Welle, R., Traum, M., Abbey, E., and Rickard, M., "A New Shock-Tube Facility for Studying Combustion Phenomena in Mixtures Containing Condensed Species," *Proceedings of NHTC'01*, National Heat Transfer Conference, Paper NHTC2001-20136, June 2001.

[12]Kee, R. J., Rupley, F. M., and Miller, J. A., "The Chemkin Thermodynamic Database," Sandia National Labs., Rept. SAND87-8215B, Albuquerque, NM, March 1990.

[13]Tanaka, H., Koshi, M., and Matsui, H., "Unimolecular Decomposition of Silane in Shock Waves," *Bulletin of the Chemical Society of Japan*, Vol. 60, Oct. 1987, pp. 3519–3523.

[14]Petersen, E. L., Rickard, M. J. A., Crofton, M. W., Abbey, E. D., Traum, M. J., and Kalitan, D. M., "A Facility for Gas- and Condensed-Phase Measurements behind Shock Waves," *Measurement Science and Technology* (in press).

[15]Skinner, G. B., and Ringrose, G. H., "Ignition Delays of a Hydrogen–Oxygen–Argon Mixture at Relatively Low Temperatures," *Journal of Chemical Physics*, Vol. 42, No. 6, 1965, pp. 2190–2192.

[16]Bowman, C. T., and Seery, D. J., "Chemiluminescence in High-Temperature Oxidation of Methane," *Combustion and Flame*, Vol. 12, No. 6, 1968, pp. 611–614.

[17]Dandy, D. S., and Vosen, S. R., "Numerical and Experimental Studies of Hydroxyl Radical Chemiluminescence in Methane–Air Flames," *Combustion Science and Technology*, Vol. 82, No. 1, 1992, pp. 131–150.

[18]Petersen, E. L., Kalitan, D. M., and Rickard, M. J. A., "Calibration and Chemical Kinetics Modeling of an OH Chemiluminescence Diagnostic," AIAA Paper 2003-4493, July 2003.

[19]Horning, D. C., Davidson, D. F., and Hanson, R. K., "Study of the High-Temperature Autoignition of n-Alkane/O_2/Ar Mixtures," *Journal of Propulsion and Power*, Vol. 18, No. 2, 2002, pp. 363–371.

[20]Kondo, S., Tokuhashi, K., Nagai, H., Iwasaka, M., and Kaise, M., "Experimental Study of Spontaneous Ignition Limit of Oxygen-Lean Silane Mixtures," *Combustion and Flame*, Vol. 97, No. 3–4, 1994, pp. 296–300.

[21]Petersen, E. L., Davidson, D. F., Röhrig, M., and Hanson, R. K., "High-Pressure Shock-Tube Measurements of Ignition Times in Stoichiometric H_2/O_2/Ar Mixtures," *Proceeding of the 20th International Symposium on Shock Waves*, edited by B. Sturtevant, J. E. Shepherd, and H. G. Hornung, World Scientific, London, 1996, pp. 941–946.

[22]Kee, R. J., Rupley, F. M., Miller, J. A., Coltrin, M. E., Grcar, J. F., Meeks, E., Moffat, H. K., Lutz, A. E., Dixon-Lewis, G., Smooke, M. D., Warnatz, J., Evans, G. H., Larson, R. S., Mitchell, R. E., Petzold, L. R., Reynolds, W. C., Caracotsios, M., Stewart, W. E., Glarborg, P., Wang, C., and Adigun, O., *Chemkin Collection*, Release 3.6, Reaction Design, Inc., San Diego, CA, 2000.

[23]Park, C., and Fujiwara, T., "Spectral Studies of $SiCl_4 + N_2O$+Ar and SiH_4+Ar Mixtures in a Shock Tube in 160–550 nm Range," *Shock Tube and Shock Wave Research, Proceedings of the Eleventh International Symposium on Shock Tubes and Waves*, edited by B. Ahlborn, A. Hertzberg, and D. Russell, Univ. of Washington Press, Seattle, WA, 1978, pp. 148–155.

[24]Petersen, E. L., and Crofton, M. W., "Measurements of High-Temperature Silane Pyrolysis Using SiH_4 IR Emission and SiH_2 Laser Absorption," *Journal of Physical Chemistry*, Vol. 107, No. 50, 2003, pp. 10988–10995.

[25]Petersen, E. L., Röhrig, M., Davidson, D. F., Hanson, R. K., and Bowman, C. T., "High-Pressure Methane Oxidation Behind Reflected Shock Waves," *Proceedings of the Combustion Institute*, Vol. 26, 1996, pp. 799–806.

[26]Petersen, E. L., Davidson, D. F., and Hanson, R. K., "Kinetics Modeling of Shock-Induced Ignition in Low-Dilution CH_4/O_2 Mixtures at High Pressures and Intermediate Temperatures," *Combustion and Flame*, Vol. 117, No. 1–2, 1999, pp. 272–290.

[27]Kalitan, D. M., and Petersen, E. L., "Evaluation of Several Chemical Kinetics Mechanisms of Silane Ignition and Oxidation at Elevated Temperatures," *Combustion and Flame* (submitted for publication).